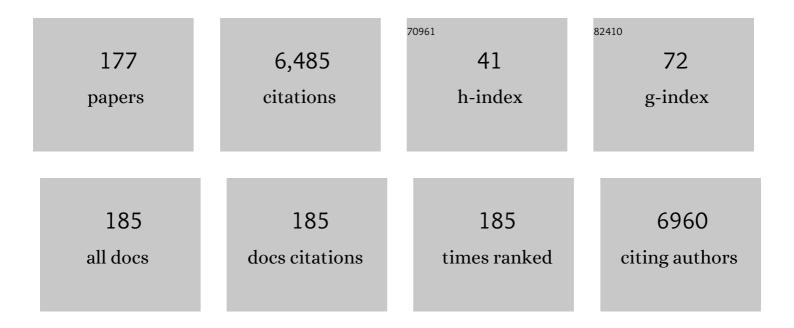
Michel L Trudeau

List of Publications by Year in descending order

Source: https://exaly.com/author-pdf/4963100/publications.pdf Version: 2024-02-01



#	Article	IF	CITATIONS
1	Current density dependence of peroxide formation in the Li–O2 battery and its effect on charge. Energy and Environmental Science, 2013, 6, 1772.	15.6	586
2	Hydrogen Storage for Mobility: A Review. Materials, 2019, 12, 1973.	1.3	461
3	Structural changes during high-energy ball milling of iron-based amorphous alloys: Is high-energy ball milling equivalent to a thermal process?. Physical Review Letters, 1990, 64, 99-102.	2.9	203
4	One-Step Overall Water Splitting under Visible Light Using Multiband InGaN/GaN Nanowire Heterostructures. ACS Nano, 2013, 7, 7886-7893.	7.3	190
5	Review and analysis of nanostructured olivine-based lithium recheargeable batteries: Status and trends. Journal of Power Sources, 2013, 232, 357-369.	4.0	173
6	Introductory remarks on nanodielectrics. IEEE Transactions on Dielectrics and Electrical Insulation, 2004, 11, 808-818.	1.8	158
7	Pyrolyzed Cobalt Phthalocyanine as Electrocatalyst for Oxygen Reduction. Journal of the Electrochemical Society, 1993, 140, 1974-1981.	1.3	131
8	A photochemical diode artificial photosynthesis system for unassisted high efficiency overall pure water splitting. Nature Communications, 2018, 9, 1707.	5.8	123
9	Low Hydrogen Overpotential Nanocrystalline Niâ€Mo Cathodes for Alkaline Water Electrolysis. Journal of the Electrochemical Society, 1991, 138, 1316-1321.	1.3	118
10	Hydrogen Storage in Chemically Reducible Mesoporous and Microporous Ti Oxides. Journal of the American Chemical Society, 2006, 128, 11740-11741.	6.6	108
11	Fabrication and properties of mechanically milled alumina/aluminum nanocomposites. Materials Science & Engineering A: Structural Materials: Properties, Microstructure and Processing, 2010, 527, 7605-7614.	2.6	106
12	Atomicâ€5cale Origin of Longâ€Term Stability and High Performance of <i>p</i> â€GaN Nanowire Arrays for Photocatalytic Overall Pure Water Splitting. Advanced Materials, 2016, 28, 8388-8397.	11.1	106
13	Microstructure and physical properties of nanostructured tin oxide thin films grown by means of pulsed laser deposition. Thin Solid Films, 2002, 419, 230-236.	0.8	103
14	Amorphous and nanocrystalline Fe–Ti prepared by ball milling. Journal of Materials Research, 1993, 8, 3059-3068.	1.2	94
15	H ₂ Storage Materials (22KJ/mol) Using Organometallic Ti Fragments as Ïf-H ₂ Binding Sites. Journal of the American Chemical Society, 2008, 130, 6992-6999.	6.6	86
16	Behavior of Solid Electrolyte in Li-Polymer Battery with NMC Cathode via in-Situ Scanning Electron Microscopy. Nano Letters, 2020, 20, 1607-1613.	4.5	85
17	XPS investigation of surface oxidation and reduction in nanocrystalline CexLa1 â^'xO2 â^'y. Surface and Interface Analysis, 1995, 23, 219-226.	0.8	83
18	Pulsed laser deposition of nanostructured tin oxide films for gas sensing applications. Sensors and Actuators B: Chemical, 2001, 77, 383-388.	4.0	79

#	Article	IF	CITATIONS
19	Nanocrystalline materials in catalysis and electrocatalysis: Structure tailoring and surface reactivity. Scripta Materialia, 1996, 7, 245-258.	0.5	73
20	Interdiffusion during the formation of amorphous alloys by mechanical alloying. Physical Review Letters, 1989, 62, 2849-2852.	2.9	72
21	Sulfated and Phosphated Mesoporous Nb Oxide in the Benzylation of Anisole and Toluene by Benzyl Alcohol. Journal of the American Chemical Society, 2006, 128, 13996-13997.	6.6	67
22	High-resolution electron microscopy study of Niî—,Mo nanocrystals prepared by high-energy mechanical alloying. Materials Science & Engineering A: Structural Materials: Properties, Microstructure and Processing, 1991, 134, 1361-1367.	2.6	64
23	Structural and magnetic characterization of granular Y ₁ Ba ₂ Cu ₃ O _{7â^î} nanocrystalline powders. Journal of Materials Research, 1994, 9, 535-540.	1.2	63
24	Nanocrystalline Fe-(Co,Ni)-Si-B: The mechanical crystallization of amorphous alloys and the effects on electrocatalytic reactions. Physical Review B, 1992, 45, 4626-4636.	1.1	62
25	New advanced cathode material: LiMnPO4 encapsulated with LiFePO4. Journal of Power Sources, 2012, 204, 177-181.	4.0	58
26	Advanced Materials for Energy Storage. MRS Bulletin, 1999, 24, 23-26.	1.7	56
27	Nanocrystalline Ni-Mo alloys and their application in electrocatalysis. Journal of Materials Research, 1994, 9, 2998-3008.	1.2	55
28	Graphitization and particle size analysis of pyrolyzed cobalt phthalocyanine/carbon catalysts for oxygen reduction in fuel cells. Journal of Materials Research, 1994, 9, 3203-3209.	1.2	54
29	Redox Properties of Nanocrystalline Cu-Doped Cerium Oxide Studied by Isothermal Gravimetric Analysis and X-ray Photoelectron Spectroscopy. Journal of Physical Chemistry B, 1999, 103, 8858-8863.	1.2	54
30	In situ high-resolution transmission electron microscopy synthesis observation of nanostructured carbon coated LiFePO4. Journal of Power Sources, 2011, 196, 7383-7394.	4.0	52
31	Sign reversal of the Hall coefficient in amorphous Ni-Zr alloys. Physical Review B, 1983, 27, 5955-5959.	1.1	51
32	Room-Temperature Ammonia Formation from Dinitrogen on a Reduced Mesoporous Titanium Oxide Surface with Metallic Properties. Journal of the American Chemical Society, 2002, 124, 9567-9573.	6.6	51
33	Evaluation of strain rate sensitivity by constant load nanoindentation. Journal of Materials Science, 2012, 47, 7189-7200.	1.7	51
34	Growth of carbon nanotubes on Ohmically heated carbon paper. Chemical Physics Letters, 2001, 342, 503-509.	1.2	50
35	Influence of Loading on the Activity and Stability of Heatâ€Treated Carbonâ€Supported Cobalt Phthalocyanine Electrocatalysts in Solid Polymer Electrolyte Fuel Cells. Journal of the Electrochemical Society, 1995, 142, 1162-1168.	1.3	49
36	Nanostructured polymer microcomposites: A distinct class of insulating materials. IEEE Transactions on Dielectrics and Electrical Insulation, 2008, 15, 90-105.	1.8	49

#	Article	IF	CITATIONS
37	Making of an Industry-Friendly Artificial Photosynthesis Device. ACS Energy Letters, 2018, 3, 2230-2231.	8.8	48
38	Phase Changes and Electronic Properties in Toroidal Mesoporous Molybdenum Oxides. Angewandte Chemie - International Edition, 1999, 38, 1471-1475.	7.2	46
39	Synthesis and Electronic Properties of Potassium Fulleride Nanowires in a Mesoporous Niobium Oxide Host. Advanced Materials, 2001, 13, 29-33.	11.1	45
40	Nanocrystalline Fe and Fe-riched Fe-Ni through electrodeposition. Scripta Materialia, 1999, 12, 55-60.	0.5	44
41	Design and Synthesis of Vanadium Hydrazide Gels for Kubas-Type Hydrogen Adsorption: A New Class of Hydrogen Storage Materials. Journal of the American Chemical Society, 2010, 132, 11792-11798.	6.6	44
42	Ultra-low cost and highly stable hydrated FePO 4 anodes for aqueous sodium-ion battery. Journal of Power Sources, 2018, 374, 211-216.	4.0	44
43	Positive Hall effect in paramagnetic amorphous Zr-Fe. Physical Review B, 1988, 37, 4499-4501.	1.1	43
44	Nanoporous twinned PtPd with highly catalytic activity and stability. Journal of Materials Chemistry A, 2015, 3, 2050-2056.	5.2	43
45	Group III-nitride nanowire structures for photocatalytic hydrogen evolution under visible light irradiation. APL Materials, 2015, 3, .	2.2	42
46	Weak-localization and Coulombic interaction effects in the low-temperature resistivity and magnetoresistivity of Y-Al metallic glasses. Physical Review B, 1986, 33, 2799-2802.	1.1	41
47	The Nature of Cobalt Species in Coâ~'ZSM-5 NO Emission Control Catalysts. The Journal of Physical Chemistry, 1996, 100, 13662-13666.	2.9	41
48	Observation of a Double Maximum in the Dependence of Conductivity on Oxidation State in Potassium Fulleride Nanowires Supported by a Mesoporous Niobium Oxide Host Lattice. Advanced Materials, 2001, 13, 561-565.	11.1	41
49	High Resolution Imaging and X-Ray Microanalysis with STEM in the FE-SEM. Microscopy and Microanalysis, 2012, 18, 390-391.	0.2	41
50	A manganese hydride molecular sieve for practical hydrogen storage under ambient conditions. Energy and Environmental Science, 2019, 12, 1580-1591.	15.6	41
51	The Role of Metal Disulfide Interlayer in Li–S Batteries. Journal of Physical Chemistry C, 2018, 122, 1014-1023.	1.5	40
52	Synthesis and Electronic Properties of Reduced Mesoporous Sodium Niobium Oxides. Advanced Materials, 2000, 12, 337-341.	11.1	39
53	Synthesis and Magnetic Tuning in Superparamagnetic Cobaltocene-Mesoporous Niobium Oxide Composites. Advanced Materials, 2000, 12, 1339-1342.	11.1	37
54	Synthesis and Characterization of a New Family of Electroactive Alkali Metal Doped Mesoporous Nb, Ta, and Ti Oxides and Evidence for an Anderson Transition in Reduced Mesoporous Titanium Oxide. Inorganic Chemistry, 2001, 40, 2088-2095.	1.9	36

#	Article	IF	CITATIONS
55	Hydride-Induced Amplification of Performance and Binding Enthalpies in Chromium Hydrazide Gels for Kubas-Type Hydrogen Storage. Journal of the American Chemical Society, 2011, 133, 15434-15443.	6.6	36
56	Hydrogen Storage in Microporous Titanium Oxides Reduced by Early Transition Metal Organometallic Sandwich Compounds. Chemistry of Materials, 2007, 19, 1388-1395.	3.2	35
57	High Capacity and High Efficiency Maple Tree-Biomass-Derived Hard Carbon as an Anode Material for Sodium-Ion Batteries. Materials, 2018, 11, 1294.	1.3	34
58	Nanostructured Gold Thin Films Prepared by Pulsed Laser Deposition. Journal of Materials Research, 2004, 19, 950-958.	1.2	33
59	Multifunctional Fe ₃ O ₄ â^`Au/Porous Silica@Fluorescein Core/Shell Nanoparticles with Enhanced Fluorescence Quantum Yield. Journal of Physical Chemistry C, 2010, 114, 18313-18317.	1.5	33
60	Electronic Properties of Novel Mixed Oxidation-State Bis-Arene Chromium Nanowires Supported by a Mesoporous Niobium Oxide Host. Advanced Materials, 2000, 12, 1036-1040.	11.1	32
61	Electrochemical Studies of Hydrogen Storage in Amorphous Ni64Zr36 Alloy. Journal of the Electrochemical Society, 1993, 140, 579-584.	1.3	31
62	Electroactive mesoporous tantalum oxide catalysts for nitrogen activation and ammonia synthesis. Chemical Communications, 2006, , 1918.	2.2	31
63	Synthesis of phase-pure Li 2 MnSiO 4 @C porous nanoboxes for high-capacity Li-ion battery cathodes. Nano Energy, 2015, 12, 305-313.	8.2	31
64	Hydrogen Absorption in Amorphous and Nano-Crystalline FeTi*. Zeitschrift Fur Physikalische Chemie, 1994, 183, 45-49.	1.4	30
65	Polymer composites with a large nanofiller content: a case study involving epoxy. IEEE Transactions on Dielectrics and Electrical Insulation, 2014, 21, 434-443.	1.8	29
66	Microscopy and microanalysis of complex nanosized strengthening precipitates in new generation commercial Al–Cu–Li alloys. Journal of Microscopy, 2014, 255, 128-137.	0.8	28
67	Mechanically alloyed nanocrystalline Niâ€Mo powders: A new technique for producing active electrodes for catalysis. Applied Physics Letters, 1991, 58, 2764-2766.	1.5	27
68	Deformation induced crystallization due to instability in amorphous FeZr alloys. Applied Physics Letters, 1994, 64, 3661-3663.	1.5	27
69	Acquisition parameters optimization of a transmission electron forward scatter diffraction system in a coldâ€field emission scanning electron microscope for nanomaterials characterization. Scanning, 2013, 35, 375-386.	0.7	27
70	Defect-engineered GaN:Mg nanowire arrays for overall water splitting under violet light. Applied Physics Letters, 2015, 106, .	1.5	27
71	The oxidation of nanocrystalline FeTi hydrogen storage compounds. Scripta Materialia, 1992, 1, 457-464.	0.5	26
72	Compositional Effects in Ru, Pd, Pt, and Rh-Doped Mesoporous Tantalum Oxide Catalysts for Ammonia Synthesis. Inorganic Chemistry, 2007, 46, 5084-5092.	1.9	26

#	Article	IF	CITATIONS
73	Sulfated Mesoporous Tantalum Oxides in the Shape Selective Synthesis of Linear Alkyl Benzene. Angewandte Chemie - International Edition, 2008, 47, 4896-4899.	7.2	26
74	Kubas-Type Hydrogen Storage in V(III) Polymers Using Tri- and Tetradentate Bridging Ligands. Journal of the American Chemical Society, 2011, 133, 4955-4964.	6.6	26
75	Nanoboxes with a porous MnO core and amorphous TiO ₂ shell as a mediator for lithium–sulfur batteries. Journal of Materials Chemistry A, 2021, 9, 4952-4961.	5.2	26
76	Electrochemical and Electrocatalytic Behavior of an Ironâ€Base Amorphous Alloy in Alkaline Solutions at 70°C. Journal of the Electrochemical Society, 1989, 136, 2224-2230.	1.3	25
77	Mesostructured Fe Oxide Synthesized by Ligand-Assisted Templating with a Chelating Triol Surfactant. Journal of Physical Chemistry B, 2004, 108, 5211-5216.	1.2	24
78	Towards a more comprehensive microstructural analysis of Zr–2.5Nb pressure tubing using image analysis and electron backscattered diffraction (EBSD). Journal of Nuclear Materials, 2009, 393, 162-174.	1.3	24
79	Multivalent Manganese Hydrazide Gels for Kubas-Type Hydrogen Storage. Chemistry of Materials, 2012, 24, 1629-1638.	3.2	24
80	Thermodynamically neutral Kubas-type hydrogen storage using amorphous Cr(<scp>iii</scp>) alkyl hydride gels. Physical Chemistry Chemical Physics, 2015, 17, 9480-9487.	1.3	24
81	Layered oxides-LiNi1/3Co1/3Mn1/3O2 as anode electrode for symmetric rechargeable lithium-ion batteries. Journal of Power Sources, 2018, 378, 516-521.	4.0	24
82	Synthesis of a Stable Metallic Niobium Oxide Molecular Sieve and Subsequent Room Temperature Activation of Dinitrogen. Advanced Functional Materials, 2002, 12, 174.	7.8	22
83	Synthesis and Performance of MOF-Based Non-Noble Metal Catalysts for the Oxygen Reduction Reaction in Proton-Exchange Membrane Fuel Cells: A Review. Nanomaterials, 2020, 10, 1947.	1.9	22
84	Application of Magnetic Resonance Techniques to the In Situ Characterization of Li-Ion Batteries: A Review. Materials, 2020, 13, 1694.	1.3	22
85	Fabrication of nanocrystalline iron-based alloys by the mechanical crystallization of amorphous materials. Scripta Materialia, 1993, 2, 361-368.	0.5	21
86	Exchange-enhanced weak-localization and electron-electron interaction in amorphous paramagnetic Zr-Fe. Physical Review B, 1988, 38, 5353-5356.	1.1	20
87	X-ray Photoelectron Spectroscopy and Magnetic Studies on the Effect of Pore Size, Wall Thickness, and Wall Composition on Superparamagnetic Cobaltocene Mesoporous Nb, Ta, and Ti Composites. Inorganic Chemistry, 2000, 39, 5901-5908.	1.9	20
88	Contribution of a New Generation Field-Emission Scanning Electron Microscope in the Understanding of a 2099 Al-Li Alloy. Microscopy and Microanalysis, 2012, 18, 1393-1409.	0.2	20
89	Titanium hydrazide gels for Kubas-type hydrogen storage. Journal of Materials Chemistry A, 2013, 1, 1947.	5.2	20
90	In Situ TEM Investigation of Electron Irradiation Induced Metastable States in Lithium-Ion Battery Cathodes: Li ₂ FeSiO ₄ versus LiFePO ₄ . ACS Applied Energy Materials, 2018, 1, 3180-3189.	2.5	20

#	Article	IF	CITATIONS
91	Magnetoresistivity studies of Zr-Mamorphous alloys (M=Ni, Co, and Fe): From superconductivity to ferromagnetism. Physical Review B, 1990, 41, 10535-10544.	1.1	19
92	Optimization of hydrogen storage capacity in silica-supported low valent Ti systems exploiting Kubas binding of hydrogen. Journal of Organometallic Chemistry, 2009, 694, 2793-2800.	0.8	19
93	Cyclopentadienyl chromium hydrazide gels for Kubas-type hydrogen storage. Chemical Communications, 2010, 46, 3206.	2.2	19
94	Application of Operando X-ray Diffractometry in Various Aspects of the Investigations of Lithium/Sodium-Ion Batteries. Energies, 2018, 11, 2963.	1.6	19
95	Multi-carbonyl molecules immobilized on high surface area carbon by diazonium chemistry for energy storage applications. Electrochimica Acta, 2019, 308, 99-114.	2.6	19
96	Hydrogen evoluton on some Ni-base amorphous alloys in alkaline solution. International Journal of Hydrogen Energy, 1989, 14, 319-322.	3.8	18
97	The crystallization of amorphous Fe60Co20Si10B10and its effect on the electrocatalytic activity for H2evolution. Journal of Applied Physics, 1990, 67, 2333-2342.	1.1	18
98	Superparamagnetic and spin glass behavior in mesoporous niobium oxide bis(cyclopentadienyl)nickel composites. Journal of Materials Chemistry, 2001, 11, 1755-1759.	6.7	18
99	Functionalized Porous Silicas with Unsaturated Early Transition Metal Moieties as Hydrogen Storage Materials: Comparison of Metal and Oxidation State. Journal of Physical Chemistry C, 2010, 114, 8651-8660.	1.5	18
100	The hall effect in paramagnetic Coî—,Zr metallic glasses. Materials Science and Engineering, 1988, 99, 187-190.	0.1	17
101	The contribution of strain and plastic deformations to the amorphization reaction of Niî—,Zr alloys by mechanical alloying. Materials Science & Engineering A: Structural Materials: Properties, Microstructure and Processing, 1991, 134, 1354-1360.	2.6	17
102	New Avenue for Limiting Degradation in NanoLi ₄ Ti ₅ O ₁₂ for Ultrafast-Charge Lithium-Ion Batteries: Hybrid Polymer–Inorganic Particles. Nano Letters, 2017, 17, 7372-7379.	4.5	17
103	Mesoporous Ta oxide reduced with bis(toluene)Ti: electronic properties and mechanistic considerations of nitrogen cleavage on the low valent surface. Dalton Transactions, 2003, , 4115-4120.	1.6	16
104	Solid-State23Na and7Li NMR Investigations of Sodium- and Lithium-Reduced Mesoporous Titanium Oxides. Inorganic Chemistry, 2006, 45, 1828-1838.	1.9	16
105	Investigation of the catalytic activities of sulfated mesoporous Ti, Nb, and Ta oxides in 1-hexene isomerization. Journal of Catalysis, 2009, 266, 1-8.	3.1	16
106	Hollow Melon‧eed‧haped Lithium Iron Phosphate Micro―and Subâ€Micrometer Plates for Lithiumâ€Ion Batteries. ChemSusChem, 2014, 7, 1618-1622.	3.6	16
107	Synthesis and Electronic Properties of Low-Dimensional Bis(benzene) Vanadium Reduced Mesoporous Niobium Oxide Composites. Inorganic Chemistry, 2001, 40, 6463-6468.	1.9	15
108	Synthesis and Electrochemistry of Li- and Na-Fulleride Doped Mesoporous Ta Oxides. Chemistry of Materials, 2004, 16, 2886-2894.	3.2	15

#	Article	IF	CITATIONS
109	Observation of TiH ₅ and TiH ₇ in Bulk-Phase TiH ₃ Gels for Kubas-Type Hydrogen Storage. Chemistry of Materials, 2013, 25, 4765-4771.	3.2	15
110	Unveiling the Cation Exchange Reaction between the NASICON Li _{1.5} Al _{0.5} Ge _{1.5} (PO ₄) ₃ Solid Electrolyte and the pyr13TFSI Ionic Liquid. Journal of the American Chemical Society, 2022, 144, 3442-3448.	6.6	15
111	Dye-sensitized InGaN nanowire arrays for efficient hydrogen production under visible light irradiation. Nanotechnology, 2015, 26, 285401.	1.3	14
112	The fcc to hcp transition induced by mechanical deformations in the Ni–Ru system. Journal of Materials Research, 1992, 7, 2412-2417.	1.2	13
113	Compositional Studies on the Electronic and Magnetic Properties of Potassium Fulleride Mesoporous Niobium Oxide Composites. Chemistry of Materials, 2002, 14, 2774-2781.	3.2	13
114	Hydrogen Storage in Mesoporous Titanium Oxideâ´'Alkali Fulleride Composites. Inorganic Chemistry, 2008, 47, 2477-2484.	1.9	13
115	¹⁷ O and ¹⁵ N Solid State NMR Studies on Ligand-Assisted Templating and Oxygen Coordination in the Walls of Mesoporous Nb, Ta and Ti Oxides. Journal of the American Chemical Society, 2008, 130, 15726-15731.	6.6	13
116	Microstructural and electrochemical investigation of functional nanostructured TiO2 anode for Li-ions batteries. Journal of Power Sources, 2012, 202, 357-363.	4.0	13
117	Boosting Ultra-Fast Charge Battery Performance: Filling Porous nanoLi4Ti5O12 Particles with 3D Network of N-doped Carbons. Scientific Reports, 2019, 9, 16871.	1.6	13
118	On high-temperature evolution of passivation layer in Li–10 wt % Mg alloy via in situ SEM-EBSD. Science Advances, 2020, 6, .	4.7	13
119	Bis(cyclopentadienyl)chromium and Bis(cyclopentadienylvanadium) Composites of Mesoporous Niobium Oxide with Pseudo-One-Dimensional Organometallic Wires in the Pores. Chemistry of Materials, 2001, 13, 4808-4816.	3.2	12
120	Unusual Conductivity Patterns in Reduced Mesoporous Titanium, Niobium, and Tantalum Oxides with One-Dimensional Potassium Fulleride Wires in the Channels. Chemistry of Materials, 2001, 13, 2730-2741.	3.2	12
121	Mesoporous tantalum oxide photocatalysts for Schrauzer-type conversion of dinitrogen to ammonia. Canadian Journal of Chemistry, 2005, 83, 308-314.	0.6	12
122	Bis(benzene) and Bis(cyclopentadienyl) V and Cr Doped Mesoporous Silica with High Enthalpies of Hydrogen Adsorption. Journal of Physical Chemistry C, 2009, 113, 17240-17246.	1.5	12
123	Compositional and2H NMR Studies of Bis(benzene)chromium Composites of Mesoporous Vanadiumâ^'Niobium Mixed Oxides. Inorganic Chemistry, 2003, 42, 335-347.	1.9	11
124	Electronic Properties and Solid-State 87Rb and 13C NMR Studies of Mesoporous Tantalum Oxide Rubidium Fulleride Composites. Chemistry of Materials, 2005, 17, 1467-1478.	3.2	11
125	A Solid-State17O NMR Study of Local Order and Crystallinity in Amine-Templated Mesoporous Nb Oxide. Angewandte Chemie - International Edition, 2007, 46, 2635-2638.	7.2	11
126	Hall effect and magnetization of amorphous FeZr alloys. Journal of Applied Physics, 1984, 55, 1939-1941.	1.1	10

#	Article	IF	CITATIONS
127	Temperature and concentration variation of the Hall coefficient in amorphous Y-Al alloys. Physical Review B, 1989, 39, 13212-13217.	1.1	10
128	A versatile method for grafting polymers onto Li4Ti5O12 particles applicable to lithium-ion batteries. Journal of Power Sources, 2019, 421, 116-123.	4.0	10
129	Concentration and temperature dependence of the Hall resistivity in FeZr glasses. Journal of Applied Physics, 1985, 57, 3207-3209.	1.1	9
130	Structural and Spectroscopic Studies on Mesoporous Tantalum Oxide–Sodium Fulleride Composites with Conducting Fulleride Columns in the Pores. Advanced Functional Materials, 2003, 13, 671-681.	7.8	9
131	Synthesis and magnetic properties of decamethylsamarocene composites of mesoporous niobium oxide. Journal of Materials Chemistry, 2003, 13, 75-79.	6.7	9
132	On the path to bulk FeH2: Synthesis and magnetic properties of amorphous iron (II) hydride. Journal of Alloys and Compounds, 2014, 590, 199-204.	2.8	9
133	Variable temperature proton conductivity of mesoporous titanium oxides doped with naphthalene sulfonate formaldehyde resin. Microporous and Mesoporous Materials, 2014, 190, 284-291.	2.2	9
134	Anisotropic electron diffusion and weak localization in Cu/Al multilayers. Physical Review B, 1993, 48, 12202-12216.	1.1	8
135	Electrochemical Studies of Amorphous Ni ₆₄ Zr ₃₆ Hydride Electrodes*. Zeitschrift Fur Physikalische Chemie, 1994, 183, 365-370.	1.4	8
136	Protection of LiFePO4 against Moisture. Materials, 2020, 13, 942.	1.3	8
137	Thermal evolution of NASICON type solid-state electrolytes with lithium at high temperature <i>via in situ</i> scanning electron microscopy. Chemical Communications, 2021, 57, 11076-11079.	2.2	8
138	Engineering nanocrystalline materials from amorphous precursors. Materials Science & Engineering A: Structural Materials: Properties, Microstructure and Processing, 1995, 204, 233-239.	2.6	7
139	Variations in nanomechanical properties of back-end Zr–2.5Nb pressure tube material. Journal of Nuclear Materials, 2013, 442, 116-123.	1.3	7
140	Determination of Binary Diffusivities in Concentrated Lithium Battery Electrolytes via NMR and Conductivity Measurements. Journal of Physical Chemistry C, 2020, 124, 24624-24630.	1.5	7
141	A low-cost and Li-rich organic coating on a Li ₄ Ti ₅ O ₁₂ anode material enabling Li-ion battery cycling at subzero temperatures. Materials Advances, 2020, 1, 854-872.	2.6	7
142	Design Parameters for Enhanced Performance of Li _{1+x} Ni _{0.6} Co _{0.2} Mn _{0.2} O ₂ at High Voltage: A Phase Transformation Study by In Situ XRD. Journal of the Electrochemical Society, 2021, 168, 100526.	1.3	7
143	Proton Conductivity of Naphthalene Sulfonate Formaldehyde Resinâ€Doped Mesoporous Niobium and Tantalum Oxide Composites. ChemSusChem, 2015, 8, 301-309.	3.6	6
144	Highâ€Pressure Raman and Calorimetry Studies of Vanadium(III) Alkyl Hydrides for Kubasâ€Type Hydrogen Storage. ChemPhysChem, 2016, 17, 822-828.	1.0	6

#	Article	IF	CITATIONS
145	The effect of non-superconducting interfaces on the electrical transport properties of high-TcY1Ba2Cu3O7-xbulk oxides. Superconductor Science and Technology, 1988, 1, 180-186.	1.8	5
146	Electrochemical properties of rapidly quenched amorphous Niî—,Zr metallic ribbons and mechanically alloyed Niî—,Zr amorphous powders. International Journal of Hydrogen Energy, 1990, 15, 287-289.	3.8	5
147	Structural transformations and metastable phases produced by mechanical deformations in the Bi–Sr–Ca–Cu–O superconducting system. Journal of Materials Research, 1993, 8, 1258-1267.	1.2	5
148	Nanostructured Materials for Gas Reactive Applications. , 2007, , 365-437.		5
149	Synthesis and electrochemical properties of mesoporous titanium oxide with polythiophene nanowires in the pores. Microporous and Mesoporous Materials, 2014, 194, 52-59.	2.2	5
150	Synthesis and Electrochemical Evaluation of Multivalent Vanadium Hydride Gels for Lithium and Hydrogen Storage. Journal of Physical Chemistry C, 2016, 120, 11407-11414.	1.5	5
151	A Solid-State 170 NMR Study of Local Order and Crystallinity in Amine-Templated Mesoporous Nb Oxide. Angewandte Chemie, 2007, 119, 2689-2692.	1.6	4
152	Determination of EDS Detection Limits of Nanoparticle Using Monte Carlo Simulations. Microscopy and Microanalysis, 2012, 18, 1016-1017.	0.2	3
153	Effect of Synthesis Parameters on the Electrochemical Properties of High‣urfaceâ€Area Mesoporous Titanium Oxide with Polypyrrole Nanowires in the Pores. ChemElectroChem, 2014, 1, 2153-2162.	1.7	3
154	Lowâ€Temperature Synthesis and Electrochemical Properties of Mesoporous Titanium Oxysulfides. ChemElectroChem, 2016, 3, 256-265.	1.7	3
155	EELS Analysis of Bulk Plasmon Harmonics of Aluminium at 30 keV. Microscopy and Microanalysis, 2018, 24, 464-465.	0.2	3
156	Dilute-antimonide GaSbN/GaN dots-in-wire heterostructures grown by molecular beam epitaxy: Structural and optical properties. Applied Physics Letters, 2021, 118, .	1.5	3
157	Spontaneous nitride formation in the reaction of mesoporous titanium oxide with bis(toluene) titanium in a nitrogen atmosphere. Studies in Surface Science and Catalysis, 2002, 141, 661-668.	1.5	2
158	Secondary Electron Yield at High Voltages up to 300 keV. Microscopy and Microanalysis, 2015, 21, 1705-1706.	0.2	2
159	Computational study of H2 binding to MH3 (M = Ti, V, or Cr). Dalton Transactions, 2019, 48, 4921-4930.	1.6	2
160	EDS of Lithium Materials from 0.5 to 30 keV. Microscopy and Microanalysis, 2021, 27, 1868-1869.	0.2	2
161	Nanostructured material induced by a 400 W yag laser. Scripta Materialia, 1997, 9, 221-224.	0.5	1
162	Highâ€resolution imaging and Xâ€ray microanalysis in the FEâ€SEM. Surface and Interface Analysis, 2014, 46, 1286-1290.	0.8	1

#	Article	IF	CITATIONS
163	UVâ€Initiated Synthesis of Electroactive High Surface Area Ta and Ti Mesoporous Oxides Composites with Polypyrrole Nanowires within the Pores. ChemNanoMat, 2015, 1, 276-284.	1.5	1
164	Synthesis and Solidâ€State NMR Studies of Protonâ€Conducting Mesoporous Niobium Oxide Polymer Composites with Nafionâ€Like Thermal Durability. ChemNanoMat, 2015, 1, 430-437.	1.5	1
165	Surface reactivity of nanocrystalline Fe87Zr7Cu1B5 alloys. Scripta Materialia, 1997, 9, 217-220.	0.5	0
166	Comparison of Partly Revealed Anisotropic Microstructures Using Grid Intersepts as Applied to Zirconium Tubes. Microscopy and Microanalysis, 2002, 8, 1304-1305.	0.2	0
167	What is the Best Beam Energy for X-Ray Microanalysis of Nanomaterials in Electron Microscopy?. Microscopy and Microanalysis, 2009, 15, 460-461.	0.2	0
168	Fe Distribution in Zr-2.5Nb Pressure Tubes Having Variable Deformation Properties. Microscopy and Microanalysis, 2009, 15, 482-483.	0.2	0
169	HR-STEM In-Situ Mechanical Testing of FIB Samples. Microscopy and Microanalysis, 2012, 18, 772-773.	0.2	0
170	EDS Spectrum Imaging with Fast Fourier Transforms. Microscopy and Microanalysis, 2012, 18, 1008-1009.	0.2	0
171	Synthesis of New Electrode Materials for Li-Ions Batteries using an Environmental HRTEM Microscopy and Microanalysis, 2012, 18, 1476-1477.	0.2	0
172	In-Situ Synthesis of New Electrode Materials for Li-Ions Batteries using a cold FEG Environmental HRTEM. Microscopy and Microanalysis, 2014, 20, 1522-1523.	0.2	0
173	Electron Dose Management for High Angle Annular Dark Field Scanning Transmission Electron Microscope Tomography of Beam Sensitive Materials. Microscopy and Microanalysis, 2016, 22, 1294-1295.	0.2	0
174	The Joy of Nanoscale Imaging and Spectroscopy in a Low Accelerating Voltage Scanning Transmitted Electron Microscope. Microscopy and Microanalysis, 2018, 24, 640-641.	0.2	0
175	EELS Monitoring of Beam-Induced Dynamic Transformation of Lithium Materials at 30 keV. Microscopy and Microanalysis, 2019, 25, 2168-2169.	0.2	0
176	Formation of Mn hydrides from bis(trimethylsilylmethyl) Mn(II): A DFT study. Polyhedron, 2020, 178, 114355.	1.0	0
177	Improvement in the Characterization of the 2099 Al-Li Alloy by FE-SEM. , 2012, , 23-28.		Ο